River Flow 2010 - Dittrich, Koll, Aberle & Geisenhainer (eds) - © 2010 Bundesanstalt für Wasserbau ISBN 978-3-939230-00-7

An estimation of gravel mobility over an alpine river gravel bar (Arc en Maurienne, France) using PIT-tag tracers

B. Camenen, J. Le Coz, A. Paquier & M. Lagouy
Cemagref Lyon, 3 bis quai Chauveau CP220, 69336 LYON cedex 09, FRANCE

ABSTRACT: Passive Integrated Transducers (PIT) tag method to trace gravel particle is increasingly used to estimate gravel movements in mountainous rivers. Reported recovery percentages after one flood are often over 80%, demonstrating the effectiveness of this technique for small mountainous rivers. We used this technique to get detailed spatial information on particle movements on a gravel bar in an alpine river (Arc en Maurienne, France). Six patches have been placed on the gravel bar (three on the bar head in August 2008 and three along the secondary channel in June 2009). During this period, the main events correspond to flushing events of the upstream dams and reservoirs by dam managers, as well as short high flow periods in May 2009 due to snow melt. Only these events have an impact on the gravel bar since it is dry for lower flows. First results with PIT-tag technique indicate a very strong erosion of the head of the bar, especially on the side of the main channel. Two sample plots have been totally eroded and marked particles have moved to the main channel after the first and the second flushing events, respectively. The secondary channel shows lower dynamics. Recovery percentages were approximately 80% after each event until marked gravels reached the main channel through the first connecting cross-channel. Travel distances were independent of the particle diameter (40 to 300mm). The downstream part of the secondary channel and the tail of the gravel bar were not affected by the last flushing event in June 2009. Most of the surface of the downstream part of the gravel bar was dry during this event as a consequence of the May 2008 flood that significantly eroded the main channel. As a first conclusion, the PIT-tag method yields interesting results for the gravel bar dynamics but the investigation domain is limited in space (and time) for our study case. Indeed, we were not able to recover PIT-tag in the main channel and downstream.

Keywords: PIT-tag, Bedload, Gravel bar, Alpine river

1 INTRODUCTION

The knowledge in river bed morphology has been of increasing importance for addressing engineering and ecological problems in rivers over recent decades. The movement of sediments along the bed of an alluvial channel is one of the key processes that needs to be understood. However, there exist only a few experimental techniques to measure bedload transport accurately. Bedload samplers yield significant uncertainty (Hubbell et al, 1985) and are difficult to set up in alpine rivers, where the flow may be supercritical. Recently, radio-tracking technique has been developed and tested on mountain rivers (Habersack, 2001 or Lamarre et al., 2005). This method allows the measurement of the travel distance of individual particles. Habersack (2001) used active transponders allowing their localisation in real time while Lamarre et al. (2005) used passive transponders allowing a location after a specific event. This paper presents some first results applying thismethod with passive transponders on a gravel bar in an alpine river where the flow is typically faster than in a mountain river.

2 PRESENTATION OF THE STUDY SITE

2.1 *Arc en Maurienne River*

The Maurienne valley, France, is characterised by a density of infrastructure (railway Lyon-Torino, national road RN6 and freeway A43) in a narrow

valley. The Arc River bed is thus strongly constrained laterally with mean slope varying downstream from S = 1 to 0.2%(Hydratec & Cemagref, 1999). In several places along the river, a system of alternate bars is observed, which is typical of laterally constrained rivers. This valley is also marked by an intense input of sediments from the catchment area, and especially of fine sediments (schist mainly) from the ArvesMountains. The catchment area is 1957 km2 (grey area in Fig. 1) with a nival hydrologic regime and a mean water discharge from 6-8 m3/s in winter to 15-20 m3/s in summer (Sainte Marie de Cuines, study site in Figure 1; Jodeau, 2007).Main floods usually occur at the beginning of summer and in autumn. The dams allow mitigation of small floods. However, because of their small capacity, they are usually open during larger floods and thus have no impact on the flood propagation in the downstream part of the valley (Marnézy, 1999). As often observed in dam reservoir studies, sediment transport is strongly affected. Fine and especially coarse sediments are stored in the reservoir. The compensation water discharge is often not strong enough to wash out sediments brought to the river by torrential tributaries.

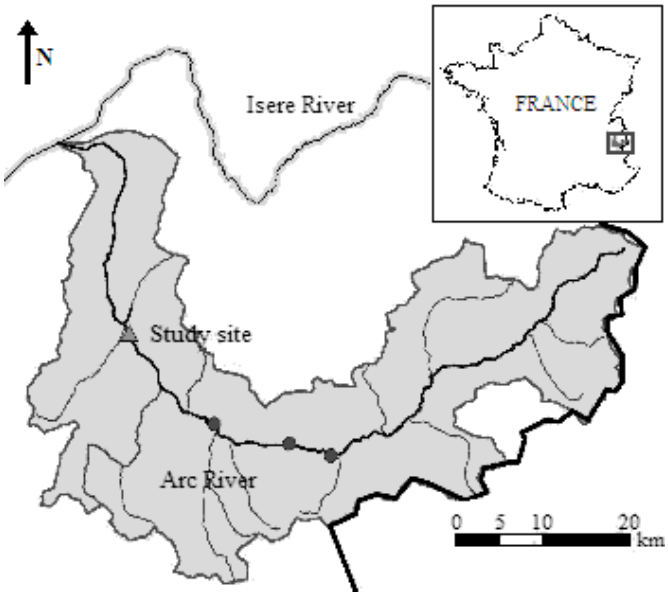

Figure 1: Localisation map of the Arc River (river dams are represented by filled circles).

2.2 *The gravel bar*

The study site is located 15 km downstream of Saint Jean de Maurienne (see Fig. 1). The gravel bar lies on the downstream part of an alternate bar system in a straight reach constrained by dykes. The monitoring of this bar started in 2005 (Jodeau, 2007; Jodeau et al., 2007, 2008) with a focus on the impact of river dam flushing on its morphodynamics. Regular topography and grain size analysis were achieved during the last four years. Since August 2008, Passive Integrated Transducers (PIT) tag method to trace gravel particle is used to estimate bedload transport over the gravel bar. Six patches have been placed on the gravel bar: patches 1, 2 and 3 on the head in August 2008, patches 4, 5, and 6 along the secondary channel in June 2009 (see Figure 2).

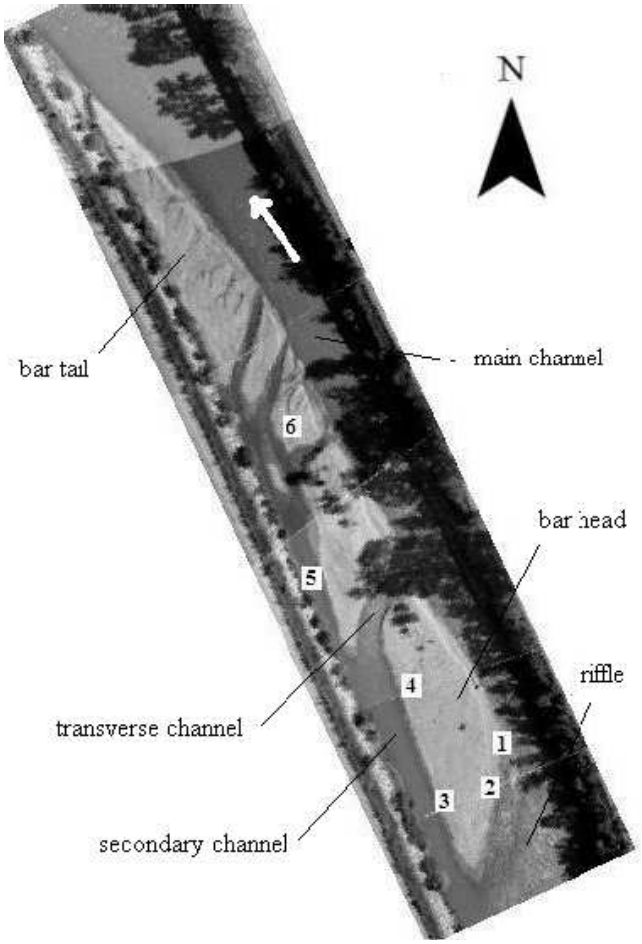

Figure 2: Image of the gravel bar taken from a drone in July 2006 (Jodeau, 2007) with the position of the 6 patches emphasized.

2.3 *Hydrology from August 2008 to August 2009*

The water discharge is estimated thanks to a pressure transducer located 200m on the downstream part of the gravel bar. Regular discharge measurements (using electromagnetic current-meter on a wading rod for low discharges or torpedo currentmeter from the bridge for larger discharges) were performed in order to establish a rating curve. The period of the study follows a 10-year return period flood that occurs in the end ofMay 2008. The maximum discharge was estimated as 500 m3/s approximately. As observed in Fig. 3, the water discharge is generally very low (6-8 m3/s) because of damregulation (compensation discharge). Because of the snow melt in spring, the discharge increases significantly during this period varying from 20 to 50m3/s (note that the station was out of order from March 20th to May

1st). The three main events observed during this period correspond to flushing events conducted by the dam managers. Two of these events correspond to a side reservoir flush in 2008, September 25th-26th and 2009, May 25th-26th (see Figure 3). The mean water discharge was approximately 70-80 m3/s with a peak at 100 m3/s (see Fig. 4). Both events last two days. However, in May 2009, the reservoir flush was foregone by large discharges from the snow melt. The third event corresponds to the river dam flush in 2009, June 8th. This event lasted approximately 12 hours with a first plateau at 80 m3/s (4 hour long) and a second plateau at 125 m3/s (3 hour long).

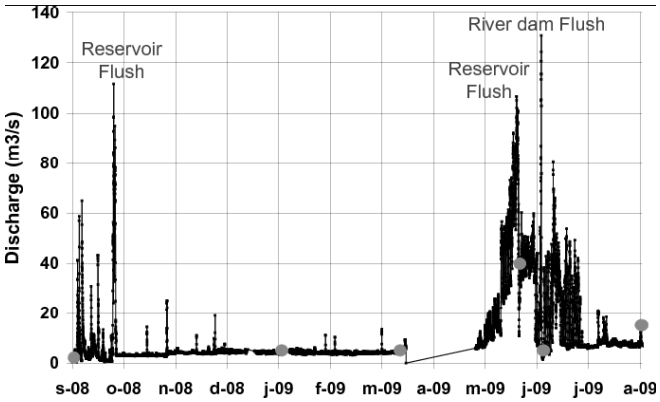

Figure 3: Water discharge at Sainte Marie de Cuines during the period of the study (field measurements are represented by filled circles).

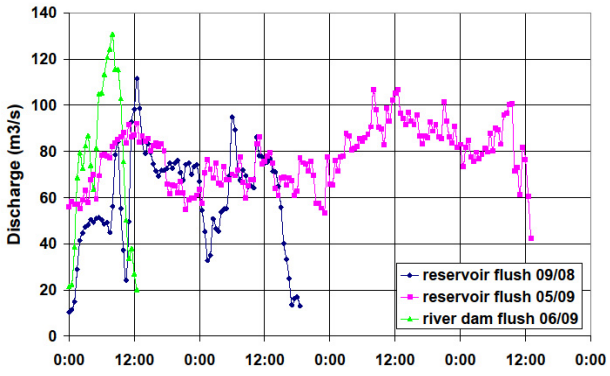

Figure 4:Water discharge at Sainte Marie de Cuines for the three main events.

3 PIT-TAG TRACERS

3.1 *Method*

The principle is to follow individually gravels tagged with Passive Integrated Transponders (PIT). PIT tags (developed by TIRIS Technology and distributed by Texas Instruments) can be inserted into holes drilled in natural particles. Then, a set of particles can be put back into the river. The search of the particles can be done with a specific antenna after each main event together with a DGPS to note the location of each particle detected. The antenna send an electromagnetic signal at a frequency of 134 Hz. Whenever a transponder is detected in the antenna field, an alarm circuit on the control module sends a loud tone and the transponder code sent from the reading unit is displayed on the Palmtop. PIT tags offer several advantages for the tracking of individual sediment particles (Lamarre et al., 2005; Allan et al, 2006). First, each transponder can be encrypted with its own unique identification code. This allows detailed analysis of individual particle movements. Second, PIT tags are robust and batteryless; they can be used in either short-term or long-term studies. Finally, they are rather inexpensive (_3Cper unit), meaning that a large number of individuals can be tagged and tracked. However, the search distance remains limited and lower than 1m. And whenever several transponders are located at the same position, the alarm circuit does not respond. This method for tracking gravel was introduced recently in France to study the dynamics of the Ain River (Rollet et al., 2008) or mountainous rivers (Liébault et al., 2009).

We used this method to estimate the gravel mobility on the gravel bar in the Arc River. We adopted a different strategy from Lamarre et al. (2005) for the tagged particle layout: patches of 50 particles were set at specific positions on the gravel bar (Lamarre et al. positioned particles individually along several cross sections). The objective of our strategy was to get a statistical observation of a set of particles with similar grain size as surrounding particles and subjected to similar hydraulic conditions. For each patch, tagged particles were laid randomly on the bed surface with the exception of patch 2 where particles were burried 20cm under the bed surface. Each patch surface was approximately 2 m2. The particle characteristics for each patch correspond to a grain-size analysis of the zone achieved previously. These characteristics are presented in Tab. 1. It should be noted that the median grain diameter d50 and sorting coefficientvalues $\left(\sigma = \sqrt{d_{84}/d_{16}}\right)$ in Tab. 1 are biased because only coarser particles are represented due to the size of the PIT tag (4×23mm), and because the b-axes of the particles were classified with sieve holes of 45, 64, 90, 128, and 181mm.

Table 1: Location of each patch in the French coordinate system "Lambert 2 étendu" (in meters) and characteristics of the patches (pnb: patch number).

pnb	setting date	location	$d_{50}[mm]$	σ
1	27/08/2008	E911253.0 N345602.3	90	1.2
2	27/08/2008	E911234.8 N345585.4	64	1.2
3	27/08/2008	E911244.0 N345584.2	64	1.4
4	27/05/2009	E911195.0 N345680.0	90	1.4
5	27/05/2009	E911159.8 N345734.2	64	1.2
6	27/05/2009	E911156.1 N345763.3	64	1.2

3.2 *Results from patches 1 and 2*

Both patches 1 and 2 disappeared totally after the first reservoir flush and second reservoir flush, respectively. After the first reservoir flush (Sept. 2008), all gravel particles from patch 1 were apparently transported into the main channel. Only one pitted gravel was found afterwards on the side of the gravel bar 10 meters from the original patch position. It should be noted that no tagged particle was recovered as soon as it reached the main channel, either because it was not accessible or because the particle travelled too far. The patch 2 (positioned 20cm underground) did not move during the first reservoir flush but disappeared totally after the second reservoir flush. Even if this result was quite disappointing, it indicated the impressive erosion occurring at the gravel bar head. The time variation of the isometric line z=450.5m is presented in Figure 5. It shows the large erosion of the gravel bar head after the three main events and explains partly why all tagged particles from patch 1 and 2 disappeared.

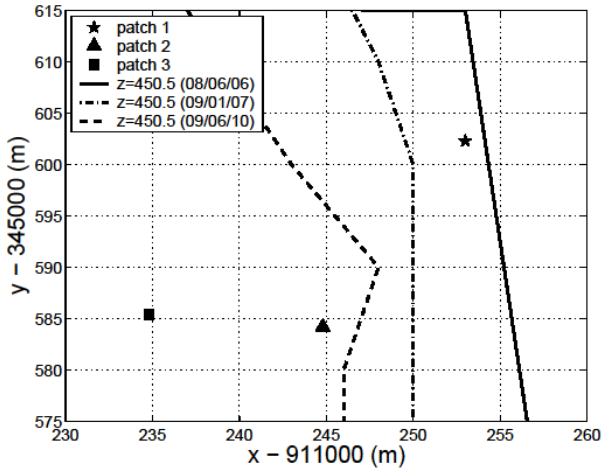

Figure 5: Location of the patches 1, 2 and 3 and time variation of the isoline z = 450.5m.

Such erosion was not observed before. It seems that the May 2008 flood (10 year return period, Q_{max} = 500m³/s) had significantly modified the shape of the gravel bar head (higher and wider). The new shape appears not to be in balance with regular hydraulic conditions.

3.3 *Results from patch 3*

Most of the tagged particles from patch 3 were recovered after the two side reservoir flushes. The recovery rate rt was always above 60% (see Tab. 2). The position of the patch (next to the secondarychannel) yielded trajectories passing along the secondary channel. It is interesting to see in Figure 6 that all particles followed a very similar trajectory. There is a large dispersion of the trajectory in the streamwise direction but it is very small in the spanwise direction. After the river dam flush, most of the tagged particles apparently reached the main channel (through the first transverse channel) and could not be recovered. Only 6 tagged particles were recovered afterwards. They were apparently trapped by a longitudinal bedform on the side of the secondary channel (cf. Figure 6).

Table 2:Mean travel distance (in metre) calculated from origin Dtm and approximated between events DDtm, and percentage of recovery.

date	07/01/2009	18/03/2009	27/05/2009	09/06/2009
D_{tm}	6.0m	5.3m	32.3m	98.2m
ΔD_{tm}	6m	0m	26m	66m
t_r	80%	60%	66%	12%

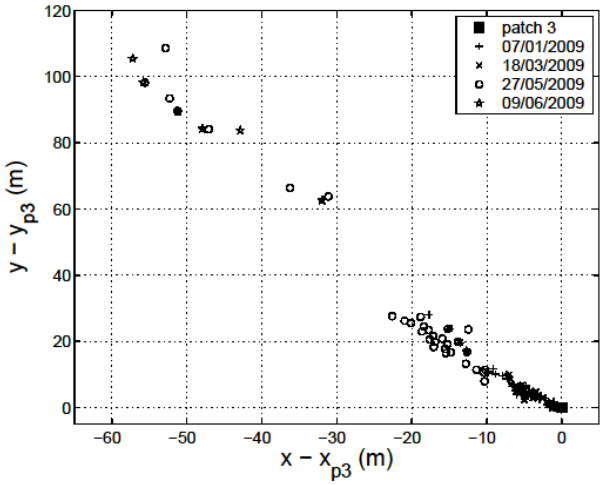

Figure 6: Position of the tagged particles of patch 3 for four research campaigns.

As bedload transport and travel distances are not linear functions of the hydrodynamic conditions, the mean travel distance of the particles was estimated as a logarithmic average:

$$D_{tm} = \exp\left[\frac{1}{n}\sum_{i=1}^{n}\ln\left(d_{t,i}\right)\right] \quad (1)$$

where n is the number of particles found. The mean travel distance ΔD_{tm} after the first reservoir flush (2008, September 25th-26th) was approximately 6m (see Tab. 2). For the second reservoir flush (2009, May 25th-26th), ΔD_{tm} was approximately 26m. It seems consistent as both events are of similar amplitude but the second one last twice longer (see Figure 4). The field campaign in March 18th showed that minor winter event produced no sediment transport over the gravel bar. It also indicates the order of uncertainties in the measurements, as D_{tm} is 70cm lower than for the January 7th campaign.

In Figure 7, the travel distance for each particle was plotted versus the grain size of the particle. As observed by Camenen & Larroudé (2003), bedload transport rate appears independent of the grain size as soon as the critical bed shear stress for inception of movement is reached. Moreover, in a mixture, the interaction between the different classes of sediment also affects significantly the critical bed shear stress of each class (Wilcock, 1997). Some influence of the grain size may be observed during the last campaign (after a period of relative low flow, see Figure 3) as all particles of small size disappeared. Only coarser particles remained since the critical bed shear stress for inception of movement was not reached

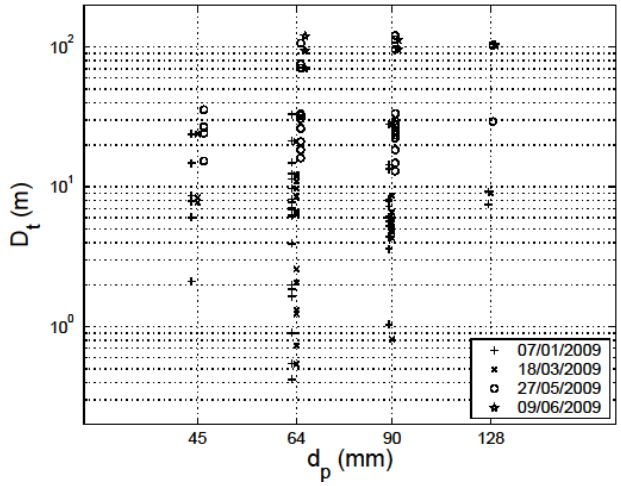

Figure 7: Travel distance of each particle as a function of the grain size.

3.4 *Results from patches 4, 5, and 6*

Patches 4, 5, and 6 were positioned just before the river dam flush in May 2009. None of the particles from these patches moved during the flushing event. Indeed, patches 4 and 5 were underwater only during the peak of discharge and velocities at these positions were apparently too low to transport sediments. Patch 6 was never underwater. For a similar peak water discharge (Q_{max} _ 120m3/s), the gravel bar was observed to be totally underwater during the flushing events in 2005, 2006 and 2007. Again, these results may be explained because of the May 2008 flood. While some sedimentation was generally observed over the gravel bar, the main channel was significantly eroded. The gravel bar is now perched and need larger water discharge to be underwater.

4 ESTIMATION OF THE GRAVEL MOBILITY

4.1 *Numerical modelling*

The model Rubar20 (Paquier, 1995) was used to simulate a simplified flushing event. It solves the 2D shallow water equations. A simplified flushing hydrograph was set upstream whereas the downstream boundary condVition was set free. The Strickler coefficient was assumed to be constant over the studied reach $K=30m^{1/3}/s$. This is consistent with the Strickler formula (1923): $K=21.2/d_{90}^{1/6} = 0.1m$.

In Figure 8, results obtained for the velocity field and water depth are presented for different times of the calculation: for a low discharge ($Q=20m^3/s$), corresponding to the compensation water, for a medium discharge ($Q=75m^3/s$), corresponding to the first plateau of the dam flush (and also to the mean discharge of the two reservoir flushes, cf. Figure 4), and for a discharge of $Q=125m^3/s$, corresponding to the maximum discharge during the dam flush. It appears that the water level significantly influences the direction and magnitude of the flow, especially in the transverse channels.

4.2 *Estimation of the bed shear stresses*

The bed shear stress was estimated from the model at six different locations that characterize the flow on the studied reach: in the main channel up to the bar head (where the flow changes from the left to the right bank, named afterwards C1tc), next to the bar head (on its narrowest part, C1up) and next to the bar tail (on its largest part, C1dn); in the secondary channel (upstream, C2up, and downstream, C2dn, to the transverse channel); and in the main transverse channel (C2tc). The bed shear stress was calculated assuming a constant Strickler coefficient $K=30m^{1/3}/s$ over the gravel bar:

$$\tau_b = \frac{\rho g U^2}{K^2 R_h^{1/3}} \qquad (2)$$

where ρ is the water density, g the acceleration of gravity, U the depth-averaged velocity, and R_h the

hydraulic radius (assumed to be equal to the water depth h).

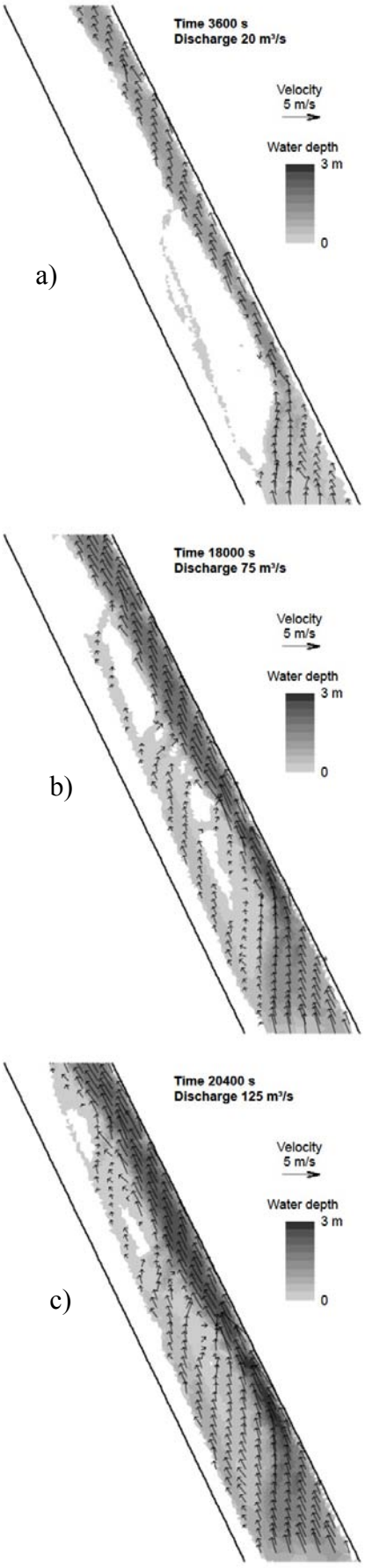

Figure 8: Water depths and velocities on the upstream part of the gravel bar simulated with the model Rubar20 for different times of the flushing event (a: t = 2hh, Q = 20m³/s; b: t = 5h, Q = 75m³/s; c: t =5h40mn, Q = 125m³/s).

In Figure 9, the bed shear stress time variations during a typical dam flushing event are plotted for the six different positions (cf. Figure 2). Because of the variability of the bed shear stress in space, these values correspond to an average of values calculated for several computational cells. It can be observed that the bed shear stress is not a linear function of the water discharge:

- In the main channel next to the bar tail (C1dn), as most of the water discharge remains in the main channel, the bed shear stress follows exactly the water discharge;
- However, next to the bar head (C1up), the width of the channel is not as large and part of the flow enters the secondary channel when Q > 50m³/s. Thus, if the bed shear stress is the highest and follows the total water discharge when Q < 100m³/s, there is a decrease of the bed shear stress when Q ≈ 125m³/s as water depth increased significantly and a significant part of the water flows in the secondary channel;
- In the main channel on the riffle up to the bar head (C1tc), one can observe a first decrease of the bed shear stress when Q ≈ 80m³/s. Indeed, for lower discharge, the flow follows the steep slope from to the left to the right bank.

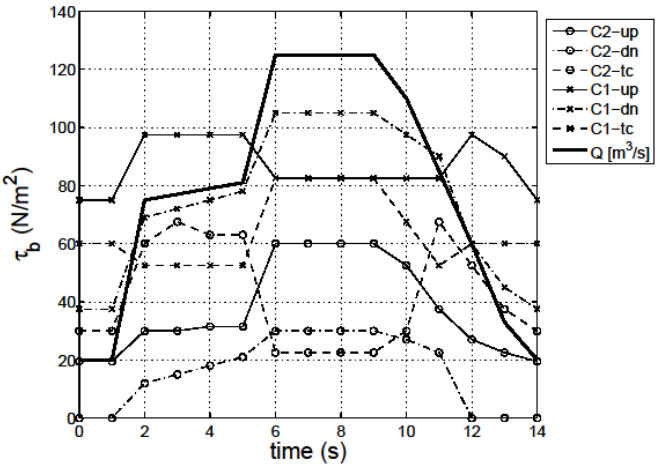

Figure 9: Bed shear stresses during the river dam flushing event obtained from the model Rubar20 for different locations on the gravel bar.

For larger discharge, the flow changes direction because of the larger water depth (streamwise) and the local slope of the flow is decreasing.

A similar observation can be made in the transverse channel (C2dn) but for a larger discharge. When Q ≈ 100m³/s, the flow changes direction from spanwise to streamwise and the local slope of the flow is decreasing.

In the upper part of the secondary channel (C2up), the bed shear stress follows the water discharge but the magnitude is two to four times smaller compared to the main channel (C1dn)

Last, in the downstream part of the secondary channel (from the transverse channel), bed shear stresses remain very low as this channel is underwater for Q > 40m3/s only and negligible part of the total discharge flows in this channel.

4.3 *Estimation of the travel distances*

Assuming that the bedload thickness is equal to the roughness height $\delta_s = k_s \approx 2d_{90}$ (Van Rijn, 1993; Camenen et al., 2006), the travel distance of the particles may be estimated as follows for a typical event:

$$D_{t,num} = \int_o^T \frac{q_s(t)}{2d_{90}} dt \quad (3)$$

where T is the length of the event, and $q_s(t)$ is the instantaneous bedload transport rate (in m3/s/m) calculated thanks to the Camenen & Larson (2005) formula. As observed in Figure 7, bedload transport appears not to be function of the grain size. Calculations were achieved for different grain sizes by calculating the critical bed shear stress based on the work of Wilcock & Crowe (2003): the critical bed shear stress for each individual class of a mixture should be not as sensitive to the grain size and

$$\frac{\tau_{cr,i}}{\tau_{cr,90}} = \left(\frac{d_i}{d_{50}} \right)^b \quad (4)$$

with b = 0.12 for $d_i/d_{50} < 1$ and b = 0.67 for $d_i/d_{50} > 1$.

These results in Tab. 3 are in agreement with experimental measurements although a large scatter exists. In the main channel, the travel distance is of the order of one to five hundred meters for a typical reservoir or dam flushing event. Even during low flow, some non-negligible bedload transport may occur. On the other hand, in the secondary channel, computed travel distances are very small. As observed thanks to the Pit-tag method, for a typical reservoir or dam flushing event, it is in the order of several meters to several tens of meters in the upstream part of the secondary channel. The suggested model tends however to underestimate the results compared to the field measurements. For a reservoir flush, the computed travel distance varies from 0.15 to 1.6m whereas the averaged measured distance is 6m (cf. Tab. 2 and 3). For a dam flush, the computed travel distance varies from 4 to 14m whereas the averaged measured distance is 66m. Nearly no sediment transport is predicted in the downstream part of the secondary channel.

Table 3: Travel distances (in metre) calculated for the three main events at different locations next to the gravel bar.

location	reservoir flush	dam flush	low flow (1day)
$d_{50} = 45$mm			
main channel	465m	249m	3.5m
2nd channel (up)	1.6m	14.3m	<0.1m
2nd channel (dn)	<0.1m	0.1m	0m
$d_{50} = 64$mm			
main channel	405m	224m	2.6m
2nd channel (up)	1.2m	12.0m	<0.1m
2nd channel (dn)	<0.1m	0.1m	0m
$d_{50} = 90$mm			
main channel	174m	116m	0.5m
2nd channel (up)	0.15m	4.1m	<0.1m
2nd channel (dn)	0m	<0.1m	0m

5 CONCLUSIONS

The PIT-tag technique to measure travel distance of individual particles was applied to a gravel bar in an alpine river. This method was fruitful in the secondary channel where approximately 80% of the tagged particles were recovered. It showed that the travel length of the particles was independent of the grain size although large dispersion was observed in the streamwise direction. A simplemodel to estimate the travel distance was suggested and yielded satisfactory results. On the other hand, it appeared that the transport in the main channel is so intense that gravels are easily transported even during low flows. As soon as tagged particles reached the main channel, it was impossible to recover them. Consequently, the PIT-tag method offered a limited spatial extent when applied to our study case.

The large erosion of the gravel bar head was suspected to be due to the major flood of May 2008, which modelled a morphology that is not in equilibrium in case of regular flood or flush events.

REFERENCES

Allan, J., R. Hart, and J. Tranquili (2006). Theuse of Passive Integrated Transponder (PIT) tags to trace cobble transport in a mixed sand-and-gravel beach on the high-energy Oregon coast, USA. Marine Geology 232, 63–86.

Camenen, B., A. Bayram, and M. Larson (2006). Equivalent roughness height for plane bed under steady flow. J. Hydraulic Eng. 132(11), 1146–1158.

Camenen, B. and P. Larroudé (2003). Comparison of sediment transport formulae for a coastal environment. Coastal Eng. 48, 111–132.

Camenen, B. and M. Larson (2005). A bedload sediment transport formula for the nearshore. Estuarine, Coastal & Shelf Science 63, 249–260.

Habersack, H. (2001). Radio-tracking gravel particles in a large braided river in new zealand: a field test of the sto-

chastic theory of bed load transport proposed by einstein.
Hydrological Processes 15, 377–391. Hubbell, D., H. Stevens, J. Skinner, and J. Beverage (1985). New approach to calibrating bed load samplers. J. Hydraulic Eng. 111(4), 677–694.
Hydratec (1999). Etude hydraulique de l'Arc en Maurienne de modane à l'isère [Hydraulic study of the Arc en Maurienne River from Modane to the Isère River]. Technical report, Association des Maires de Maurienne / Cemagref. (in French).
Jodeau, M. (2007). Morphodynamique d'un banc de galets en rivière aménagée lors de crues [Gravel bar morphodynamics in an engineered river during high flow events].
Ph. D. thesis, Claude Bernard University, JodeLayuo,nMI..,(Ain. HFraeunecth,)A. . Paquier, J. Le Coz, and G. Dramais (2008). Application and evaluation of LS-PIV technique for the monitoring of river surface velocities in high flow conditions. Flow Measurement & Instrumentation 19, 117–127.
Jodeau, M., A. Paquier, A. Hauet, J. Le Coz, F. Thollet, and T. Fournier (2007). Effect of a reservoir release on the morphology of a gravel bar: field observations and 2DH modeling. In River, Coastal and Estuarine Morphodynamics, Utrecht, The Netherlands.
Lamarre, H., B. Mac Vicar, and A. Roy (2005). Using passive integrated transponders (PIT) tags to investigate sediment transport in gravel-bed rivers. J. Sedimentary Res. 75,736–741.
Liébault, F., M. Chapuis, H. Bellot, and M. Deschatres (2009, April). A radio-frequency tracing experiment of bedload transport in a small braided mountain stream. In European Geosciences Union General Assembly, Vienna, Autria.
Marnézy, A. (1999). L'Arc et sa vallée, Anthropisation et géodynamique d'une rivère alpine dans son bassin versant [The Arc River and its valley, Anthropization and geodynamics of an alpine river in its catchment area]. Ph. D. thesis, Joseph Fourier University, Grenoble I, France. (in French).
Paquier, A. (1995). Modélisation et simulation de la propagation de l'onde de rupture de barrage [Modelling and simulating the propagation of dam-break wave]. Ph. D. thesis, Université Jean Monnet, Saint Etienne, France. (in French).
Rollet, A.-J., B. Mac Vicar, H. Piégay, and A. Roy (2008). L'utilisation de transpondeurs passifs pour l'estimation du transport sédimentaire : premiers retours d'expérience [a comparative study on the use of passive integrated transponders to estimate sediment transport : first results]. La Houille Blanche 4, 110–116. (in French).
Strickler, A. (1923). Contributions to the questions of velocity formulations and roughness values for rivers, canals, and closed ducts [beiträge zur frage der geschwindigkeitsformel und der rauhigkeitszahlen für ströme, kanäle und geschlossene leitungen]. Mitteilung 16, Amt für Wasserwirtschaft, Bern, Switzerland. (in German).
Van Rijn, L. (1993). Principles of sediment transport in rivers, estuaries and coastal seas. The Netherlands: Aqua Publications. Wilcock, P. (1997). The coponents of fractional transport rate. Water Resources Res. 33(1), 247–258.
Wilcock, P. and J. Crowe (2003). Surface-based transport model for mixed-size sediment. J. Hydraulic Eng. 129(2), 120–128.